

## The Remanent Magnetization of Unstable Keuper Marls

K. M. Creer

*Phil. Trans. R. Soc. Lond. A* 1957 **250**, 130-143

doi: 10.1098/rsta.1957.0016

### Email alerting service

Receive free email alerts when new articles cite this article - sign up in the box at the top right-hand corner of the article or click [here](#)

To subscribe to *Phil. Trans. R. Soc. Lond. A* go to: <http://rsta.royalsocietypublishing.org/subscriptions>

## V. THE REMANENT MAGNETIZATION OF UNSTABLE KEUPER MARLS

By K. M. CREER

Measurements of the directions and intensities of magnetization of Keuper Marls from Sidmouth are described. The natural remanent magnetization of these rocks is shown to be unstable in the geomagnetic field.

Certain laboratory experiments are described which show the natural remanent magnetization to consist of three components, a *primary* component created on, or soon after, deposition, in the same direction as that of the natural remanent magnetization of Keuper Sandstones and Marls described by Clegg, Almond & Stubbs (1954); a *secondary* component in the direction of a geocentric axial dipole field in Britain acquired since the last reversal of the main field and a temporary component built up by the geomagnetic field between collection and measurement.

The temporary and secondary components are believed to be isothermal remanent magnetizations and to be due to the red haematite cement. Application of Néel's theory of the magnetization of small single-domain particles shows that haematite grains of less than  $0.15 \mu$  in diameter will be magnetically unstable. The temporary and secondary components of magnetization are explained in terms of Néel's theory.

A suggested test of stability is described.

### CONTENTS

|   | PAGE |   | PAGE |
|---|------|---|------|
| 1. BRIEF ACCOUNT OF THE GEOLOGY   | 130  | 8. THE SECONDARY COMPONENT CONSIDERED AS AN I.R.M.                            | 139  |
| 2. THE ORIGINAL MEASUREMENTS OF THE N.R.M.  | 131  | 9. DECAY OF TEMPORARY COMPONENT DURING MEASUREMENT                            | 140  |
| 3. RE-MEASUREMENT OF THE N.R.M.   | 133  | 10. STABILITY OF THE SECONDARY COMPONENT                                      | 140  |
| 4. PRIMARY AND SECONDARY COMPONENTS OF MAGNETIZATION                                    | 136  | 11. NÉEL'S THEORY OF THE MAGNETIZATION OF SMALL SINGLE-DOMAIN PARTICLES       | 140  |
| 5. APPLICATION OF THE THREE-COMPONENT HYPOTHESIS TO OTHER TRIASSIC SANDSTONES AND MARLS | 136  | 12. INTERPRETATION OF THE TEMPORARY AND SECONDARY COMPONENTS OF NÉEL'S THEORY | 141  |
| 6. SOME PROPERTIES OF THE I.R.M. PRODUCED BY SMALL FIELDS AT ROOM TEMPERATURE           | 138  | 13. CONTRIBUTION TO N.R.M. OF GRAINS HAVING VERY HIGH RELAXATION TIMES        | 142  |
| 7. THE TEMPORARY COMPONENT CONSIDERED AS AN I.R.M.                                      | 139  | 14. A SUGGESTED TEST OF STABILITY   | 143  |
|   |      | REFERENCES  | 143  |

#### 1. BRIEF ACCOUNT OF THE GEOLOGY

New Red Sandstone rocks form the cliffs between Paignton and Sidmouth in Devonshire. They are on the whole unfossiliferous and have been separated into Permian and Triassic only by their sequence and lithology. They have been described by Ussher (1876) and Irving (1888), and more recently by Dewey (1948). The generally accepted age for the Keuper is about 190 million years.

## MAGNETIZATION OF UNSTABLE KEUPER MARLS

131

Exposed in the cliffs to the east of Sidmouth are massive bedded Keuper Marls containing gypsum. They are mostly bright red owing to the presence of a haematite cement, but green and mottled beds also occur. The beds dip towards the east at a few degrees so that a stratigraphical section of more than 100 ft. may be sampled by walking along the beach.

During the spring and summer of 1953, thirty-five orientated samples were collected from the cliff of Keuper Marl immediately to the east of Sidmouth bay.

## 2. THE ORIGINAL MEASUREMENTS OF THE N.R.M.

The direction and intensity of the natural remanent magnetization (n.r.m.) of cylindrical disks cut from the rock samples were measured on the Cambridge astatic magnetometer. At a sensitivity of about  $1.8 \times 10^{-8}$  G mm<sup>-1</sup> at 5 m, deflexions of the order of 1 cm were obtained with the disks 4 cm below the lower magnet of the astatic pair.

The mean directions of magnetization of the samples are given in table 1, together with their stratigraphic separation. The following symbols are used:  $D_s$ ,  $I_s$ , the declination

TABLE 1

| strati-<br>graphic<br>position<br>relative<br>to base<br>(ft.) | direction of n.r.m. |       | $\alpha_s$ | $\kappa_s$ | $N$ | $M$<br>( $10^{-7}$ G) |
|--|---------------------|-------|------------|------------|-----|-----------------------|
|  | $D_s$               | $I_s$ |            |            |     |                       |
| 170  | N 28° E             | +41°  | 14°        | 31         | 5   | 0.5                   |
| 145  | N 19° E             | +70°  | 9°         | 46         | 7   | 3.5                   |
| 143½   | N 23° E             | +52°  | 3°         | 276        | 9   | 2.4                   |
| 143  | N 35° E             | +40°  | 8°         | 64         | 6   | 3.2                   |
| 142½   | N 28° E             | +47°  | 3°         | 320        | 9   | 3.4                   |
| 142  | N 24° E             | +60°  | 5°         | 666        | 3   | 3.5                   |
| 134  | N 28° E             | +49°  | 5°         | 87         | 15  | 2.9                   |
| 128  | N 29° E             | +67°  | 7°         | 68         | 18  | —                     |
| 127½   | N 12° E             | +76°  | 11°        | 37         | 7   | 8.5                   |
| 119½   | N 17° E             | +66°  | 5°         | 375        | 4   | 5.3                   |
| 115½   | N 22° E             | +56°  | 5°         | 136        | 7   | 3.8                   |
| 111½   | N 28° E             | +60°  | 4°         | 87         | 14  | 4.1                   |
| 111  | N 24° E             | +44°  | 4°         | 167        | 16  | 2.8                   |
| 109½   | N 27° E             | +60°  | 9°         | 21         | 14  | 5.0                   |
| 108½   | N 19° W             | +81°  | 7°         | 25         | 18  | 5.1                   |
| 107  | S 33° W             | +85°  | —          | —          | 1   | 15.1                  |
| 106  | S 55° W             | +64°  | 18°        | —          | 3   | 3.7                   |
| 105  | S 60° W             | +67°  | 14°        | 18         | 8   | 3.0                   |
| 103  | S 12° W             | +77°  | 9°         | 25         | 12  | 3.6                   |
| 91½  | S 13° W             | +49°  | 6°         | 40         | 17  | 2.8                   |
| 91   | S 35° W             | +31°  | 5°         | 42         | 32  | 2.0                   |
| 90½  | S 36° W             | +55°  | 4°         | 66         | 26  | 2.4                   |
| 90   | S 39° W             | +45°  | 8°         | 45         | 8   | 2.3                   |
| 89½  | S 54° W             | +51°  | 9°         | 36         | 8   | 2.2                   |
| 88½  | S 18° W             | +67°  | 16°        | 35         | 4   | 2.3                   |
| 84   | S 49° W             | +45°  | 15°        | 17         | 6   | 2.7                   |
| 83   | S 50° W             | +70°  | —          | —          | 3   | 4.3                   |
| 77   | S 51° W             | +37°  | 32°        | 15         | 3   | 2.7                   |
| 72   | S 44° W             | +75°  | —          | —          | 2   | 7.2                   |
| *52  | S 37° W             | +19°  | —          | —          | 1   | 0.6                   |
| †50  | N 23° W             | +84°  | 10°        | 31         | 8   | 16.0                  |
| *48  | N 84° W             | +58°  | —          | —          | 1   | 0.8                   |
| 35   | N 30° E             | +73°  | 10°        | 25         | 11  | 15.4                  |
| 15   | N 78° E             | +86°  | 8°         | 31         | 12  | 27.0                  |
| 0  | N 13° E             | +76°  | 4°         | 214        | 7   | 7.5                   |

\* Indicates a green marl or sandstone.

† This specimen comes from beach level and 15 ft. W of a wall built into the cliff.

and inclination respectively of the n.r.m. vector;  $\alpha_s$  the radius of the cone of confidence surrounding the mean direction of magnetization and within which it is 95% probable that the true direction lies;  $\kappa_s$  the precision;  $N$  the number of disks cut from a sample;

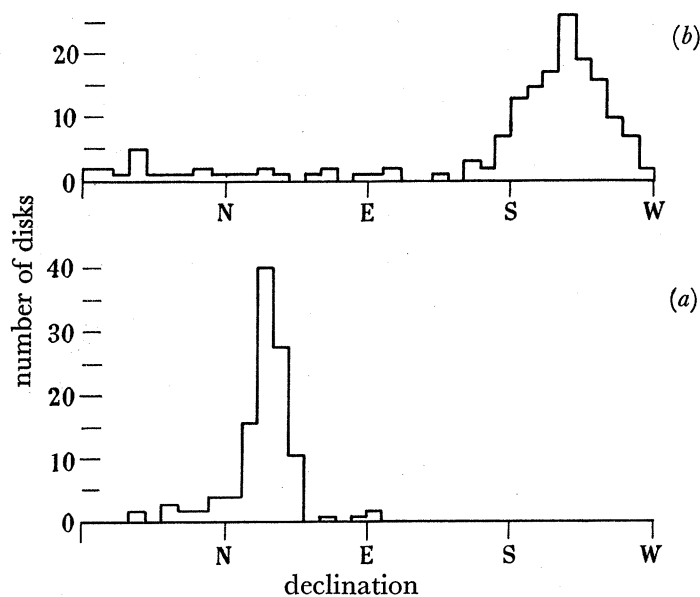


FIGURE 1. Histograms of the declinations of the n.r.m. of disks of Sidmouth Keuper Marl. (a) Upper part of the cliff; (b) lower part.

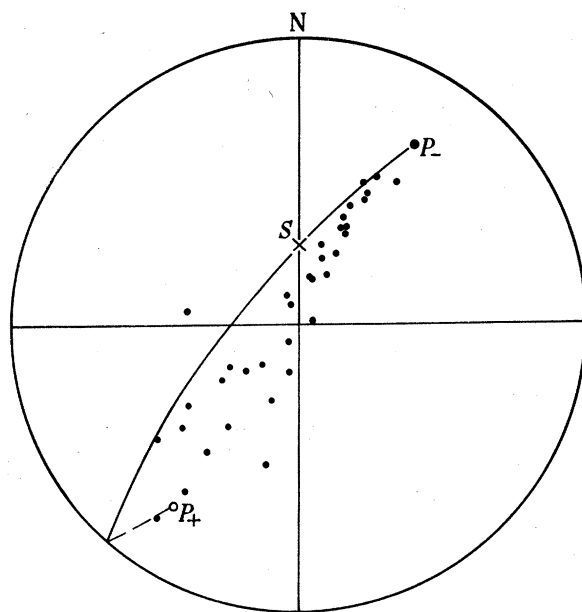


FIGURE 2. Polar equal-area projection of the mean directions of the n.r.m. of samples of Sidmouth Keuper Marl.  $S$  is the direction of an axial dipole field along the present geographical axis;  $P_-$ ,  $P_+$  are the directions of the *primary* axis of magnetization. The directions of magnetization are spread out about the great circle  $P_-SP_+$ . North-seeking poles plotted.

and  $M$  the intensity of magnetization. In all the equal-area projections the direction of the north-seeking poles of magnetization are plotted.

The frequency distribution of the declinations of individual disks is illustrated in the histograms in figure 1. The declinations found from disks from the upper part of the cliff

are all east of north and from the lower part of the cliff west of south. Consideration of the declinations alone seems to indicate that the upper and lower parts of the cliff are oppositely magnetized. However, the inclination of the n.r.m. is positive (north pole below the lower surface of the bedding planes) for all the samples as seen in figure 2.

Table 2 compares the mean values of the declinations and inclinations of these rocks with those calculated as follows by the present author from observations of the n.r.m. of stable Triassic rocks by Clegg, Almond & Stubbs (1954). The mean direction of n.r.m. ( $P_n$ ) of the normal sites has been obtained by treating the mean directions of magnetization of each of the sites as single observations.  $P_r$  has similarly been found for the four reversely magnetized sites. The axis  $P_+P_-$  is that given by rotating the reversed directions through  $180^\circ$  and finding the mean direction from all nine sites. Directions of magnetization calculated in this way are denoted by the usual symbols with the suffix  $m$ .

A suggested explanation of the observation that the horizontal components of the magnetization of the upper and lower parts of the cliff are more nearly opposed than the total intensities is given in this paper.

TABLE 2

|  | $D_m$          | $I_m$        | $\alpha_m$        | $K_m$ |
|--|----------------|--------------|-------------------|-------|
| upper levels of Sidmouth cliff                       | N $26^\circ$ E | + $57^\circ$ | $6^\circ*$        | 48    |
| lower levels of Sidmouth cliff                       | S $41^\circ$ W | + $64^\circ$ | $8^\circ*$        | 15    |
| mean direction of Clegg's 5 normal sites ( $P_n$ )   | N $29^\circ$ E | + $34^\circ$ | $10^\circ\dagger$ | 58    |
| mean direction of Clegg's 4 reversed sites ( $P_r$ ) | S $39^\circ$ W | - $16^\circ$ | $27^\circ\dagger$ | 13    |
| primary axis $P_-$                                   | N $34^\circ$ E | + $26^\circ$ | $12^\circ\dagger$ | 18    |
| $P_+$  | S $34^\circ$ W | - $26^\circ$ |                   |       |

\* Appropriate to the dispersion of sample directions within the site.

† Appropriate to the dispersion of site directions within the geological period.

### 3. RE-MEASUREMENT OF THE N.R.M.

Preliminary experiments had shown that both the intensity and direction of the n.r.m. changed with time when the disks were left in the laboratory in the geomagnetic field for times as short as a few days. It was also clear that the rate of change of the direction of magnetization decreased with time, eventually becoming zero if the specimen was kept at a fixed orientation in the earth's field. But no disk became completely remagnetized in the direction of the geomagnetic field. It was inferred therefore that there are at least two components of magnetization: a 'soft' component rapidly becoming remagnetized along the geomagnetic field when the orientation of the sample with respect to the field has been changed, and another 'hard' or stable component. It proves possible to determine the direction of this stable component and the intensities of both components. More detailed experiments were carried out on a few disks and these are described below. The experiments were carried out 15 months after collection, after the disk had been stored in field-free space for 12 months. It was first placed in a fixed position for 10 days and then, to age the soft component, it was placed in field-free space for 1 h. The direction and intensity of magnetization were then measured. This procedure was carried out six times with the disk in different orientations. In figure 3 the measured directions of magnetization,  $R_1, R_2, R_3$ , etc., for a typical disk are plotted with respect to a fixed direction in the disk. The vectors  $\mathbf{T}$  represent the successive temporary or 'soft' components built up by the geomagnetic

field, the directions of which are shown by the points **T** in figure 3. The supposed stable component is denoted by **C**, and the resultant vector  $\mathbf{R} = \mathbf{T} + \mathbf{C}$ . Since **R**, **T** and **C** must lie in a plane their projected directions must lie on a great circle. Six great circles have been drawn through corresponding pairs of points  $R_i$  and  $T_i$  giving fifteen points of intersection which are listed in table 3. The mean of these points gives the mean direction of the vector **C** which is shown in figure 4 with the circle of confidence, drawn at the 69 % probability level so as to be comparable with the standard errors quoted below.

TABLE 3. POINTS OF INTERSECTION OF GREAT CIRCLES  $R_i T_i$  AND  $R_j T_j$ 

| <i>i</i>                   | <i>j</i> | <i>D</i> | <i>I</i> |
|----------------------------|----------|----------|----------|
| 1                          | 2        | S 83° W  | +22°     |
| 1                          | 3        | S 60° W  | +28°     |
| 1                          | 4        | S 44° W  | +29°     |
| 1                          | 5        | S 46° W  | +29°     |
| 1                          | 6        | S 54° W  | +29°     |
| 2                          | 3        | S 64° W  | +30°     |
| 2                          | 4        | S 40° W  | +32°     |
| 2                          | 5        | S 45° W  | +32°     |
| 2                          | 6        | S 55° W  | +32°     |
| 3                          | 4        | S 51° W  | +23°     |
| 3                          | 5        | S 49° W  | +22°     |
| 3                          | 6        | S 51° W  | +22°     |
| 4                          | 5        | S 48° W  | +25°     |
| 4                          | 6        | S 51° W  | +22°     |
| 5                          | 6        | S 50° W  | +18°     |
| mean point of intersection |          | S 53° W  | +27°     |

radius of confidence:  $\alpha = 4^\circ$  for  $P = 0.21$

TABLE 4. SUCCESSIVE DIRECTIONS OF MAGNETIZATION OF AN UNSTABLE KEUPER MARL DISK

| orientation<br>no. | direction of <i>R</i> |          | $\psi$ | $\beta$ | <i>T/C</i> | intensity<br>( $10^{-7}$ G) |          |          |
|--------------------|-----------------------|----------|--------|---------|------------|-----------------------------|----------|----------|
|                    | <i>D</i>              | <i>I</i> |        |         |            | <i>R</i>                    | <i>T</i> | <i>C</i> |
| 1                  | S 81° W               | +24°     | 134°   | 28°     | 0.488      | 2.52                        | 1.65     | 3.38     |
| 2                  | S 14° W               | +31°     | 142°   | 31°     | 0.551      | 1.74                        | 1.45     | 2.63     |
| 3                  | S 36° W               | +11°     | 64°    | 20°     | 0.492      | 5.51                        | 2.10     | 4.25     |
| 4                  | S 62° W               | +11°     | 60°    | 19°     | 0.497      | 5.20                        | 1.94     | 3.92     |
| 5                  | S 56° W               | -6°      | 97°    | 29°     | 0.523      | 4.83                        | 2.37     | 4.53     |
| 6                  | S 59° W               | +43°     | 48°    | 17°     | 0.567      | 3.96                        | 1.56     | 2.75     |

The intensities of **T** and **C** should be the same for all six orientation positions. Figure 5 is a vector diagram for **C**, **R** and **T**.  $\psi$  is the angle between **C** and **T**,  $\beta$  the angle between **R** and **C**. We have:

$$R/T = \sin \psi / \sin \beta, \quad (3.1)$$

$$T/C = \sin \beta / \sin (\psi - \beta), \quad (3.2)$$

$$R/C = \sin \psi / \sin (\psi - \beta). \quad (3.3)$$

$\psi$  and  $\beta$  were graphically determined using the calculated mean direction of **C**. In table 4, the successive directions of **R**, the corresponding values for  $\psi$  and  $\beta$ , the ratio  $T/C$  and the intensities of **R**, **T** and **C** are given. The intensities of **R** were measured by means of the

magnetometer, those of **T** and **C** have been calculated. Average values for  $T/C$ ,  $T$  and  $C$  for the six separate determinations are given below with their standard errors:

$$T/C = 0.520 \pm 0.014,$$

$$T = 1.85 \pm 0.15 \times 10^{-7} \text{ G},$$

$$C = 3.58 \pm 0.32 \times 10^{-7} \text{ G}.$$

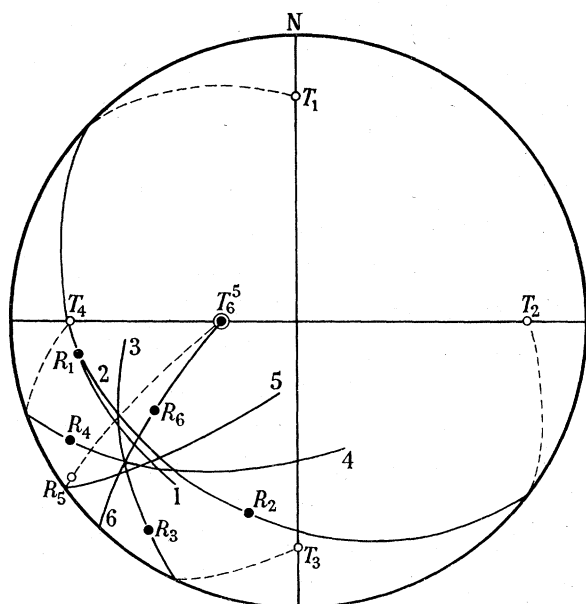


FIGURE 3

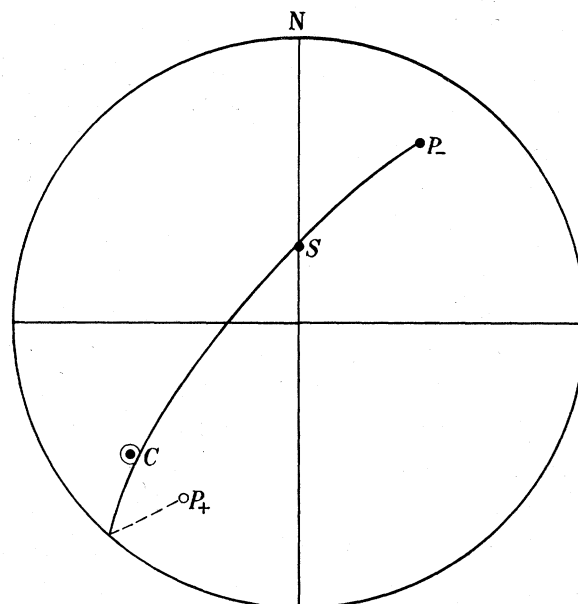
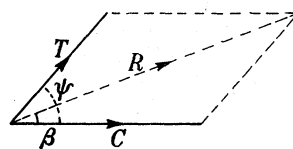


FIGURE 4

FIGURE 3. The *stable* and *temporary* components of magnetization of a typical Keuper Marl rock disk.

The points  $R_i$  represent the measured resultant directions of magnetization; the points  $T_i$  represent the corresponding directions of the geomagnetic field with respect to a fixed orientation in the disk. From the points of intersection of the great circles  $R_i T_i$  the direction of a *stable* component of magnetization is calculated.  $\text{---}\bullet\text{---}$ , great circles and directions in lower hemisphere;  $\text{---}\circ\text{---}$ , in upper hemisphere.

FIGURE 4. The *primary* and *secondary* components of magnetization of a Keuper Marl rock disk.  $S$  is the direction of an axial dipole field along the present geographical axis, and consequently of the secondary vector of magnetization.  $P$  is the direction of the *primary* magnetic vector. The calculated direction  $C$  of the *stable* component of magnetization is observed to lie close to the great circle,  $P_+ SP_-$ . The circle of confidence at the 69% probability level is shown.

FIGURE 5. The *stable*, *resultant* and *temporary* vectors of magnetization.

It is reasonable to conclude that the n.r.m. of this Keuper Marl disk consists of a stable and a temporary component of magnetization. Other disks have behaved in a similar manner, though detailed experiments have been carried out only on a few disks. It appears that the ratio  $T/C$  varies slightly between disks from one sample but considerably between samples.

## 4. PRIMARY AND SECONDARY COMPONENTS OF MAGNETIZATION

The direction of the stable component  $\mathbf{C}$  differs appreciably from the directions  $P_-$  and  $P_+$  calculated as described in § 2 for the stable Triassic rocks examined by Clegg *et al.* (1954) (see table 2).

The essential difference between the properties of the n.r.m. of the Sidmouth marls and the stable marls and sandstones is that the former possess an appreciable 'soft' component whilst the latter do not. The possibility is now examined that the Sidmouth marls have had an additional component built up *in situ*, since the time when the geomagnetic field last assumed its present (normal) sense. Such a component will be henceforth termed the *secondary* ( $S$ ) component.

Hospers (1953, 1954) shows from a study of the Tertiary and Quaternary basaltic lava flows of Iceland that the geomagnetic field, averaged over periods of tens of thousands of years, may be thought of as being produced by a geocentric dipole along the present geographic axis. The secondary component is therefore presumed to be directed along such a field for Great Britain. The vector  $\mathbf{C}$  is taken to be the sum of two vectors  $\mathbf{P}_+ + \mathbf{S}$ .  $\mathbf{P}_+$ , a *primary* component of magnetization acquired on or soon after deposition is taken to be that given in table 2. Since  $\mathbf{C} = \mathbf{P}_+ + \mathbf{S}$ ,  $C$  should lie on the great circle joining  $P_+$  and  $S$ , which is shown to be true within the experimental limits of error in figure 3. The angle between  $P_+$  and  $C$  is  $55^\circ$  and between  $P_+$  and  $S$  is  $132^\circ$ . Thus  $P_+/C = \sin 77^\circ / \sin 48^\circ = 1.31 \pm 0.09$  and  $S/C = \sin 55^\circ / \sin 48^\circ = 1.10 \pm 0.09$ , the standard errors having been obtained using the result that the radius of the circle of confidence around  $\mathbf{C}$  is  $4^\circ$ . The n.r.m. of this particular sample of Sidmouth marl can therefore be considered to be the vector sum of three components of magnetization, a primary, a secondary and a temporary:

$$\mathbf{R} = \mathbf{P} + \mathbf{S} + \mathbf{T}. \quad (4.1)$$

Since  $C = (3.58 \pm 0.32) \times 10^{-7}$  G,

we have  $P = (4.69 \pm 0.53) \times 10^{-7}$  G (*primary component*),

$S = (3.94 \pm 0.52) \times 10^{-7}$  G (*secondary component*),

$T = (1.85 \pm 0.15) \times 10^{-7}$  G (*temporary component* built up during 10 days).

In figure 2 the measured directions of the n.r.m. of the thirty-five samples are observed to lie close to the great circle  $P_+S$ , the scatter of the points along it indicating different ratios  $S/P$  for the various specimens. The scatter of directions about this great circle is considered to be due to the existence of temporary components of magnetization which were built up during the time between collection and measurement.

## 5. APPLICATION OF THE THREE-COMPONENT HYPOTHESIS TO OTHER TRIASSIC SANDSTONES AND MARLS

It is interesting to note that the averaged normal and reversed directions ( $P_n$  and  $P_r$ ) in table 2 are not exactly opposed. This could, perhaps, be due to the fact that the supposed opposed fields during the Triassic were not exactly at  $180^\circ$  to each other. However, it is more reasonable to attribute the imperfect opposition of the directions  $P_n$  and  $P_r$  to the presence in these rocks of a *small* secondary component. In figure 6,  $P_-$  and  $P_+$ , the primary



components of magnetization, and  $S$ , the geocentric axial dipole field in Great Britain are plotted. The directions  $P_n$  and  $P_r$  lie very close indeed to the great circle connecting  $P_-$ ,  $S$  and  $P_+$ , and the displacements of  $P_n$  from  $P_-$  and of  $P_r$  from  $P_+$  are in the expected sense.

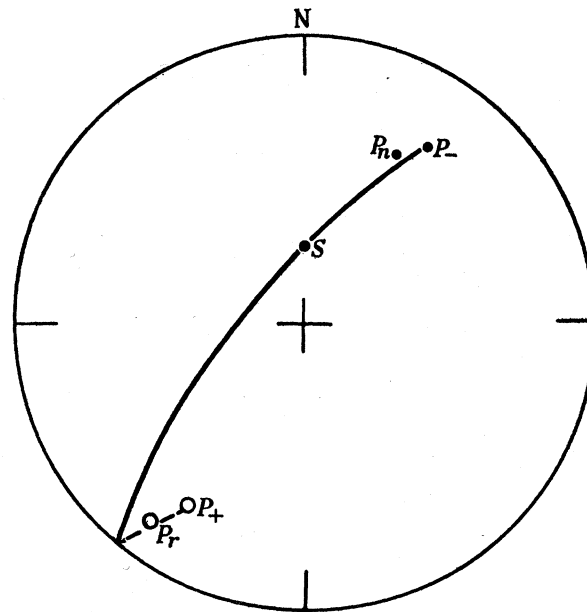


FIGURE 6. The mean directions of magnetization  $P_n$  and  $P_r$  of stable Keuper Marls.  $P_-$  and  $P_+$  are the directions of the primary axis;  $S$  is the direction of an axial dipole geomagnetic field. The directions  $P_n$  and  $P_r$  are observed to lie near the great circle  $P_-SP_+$ .

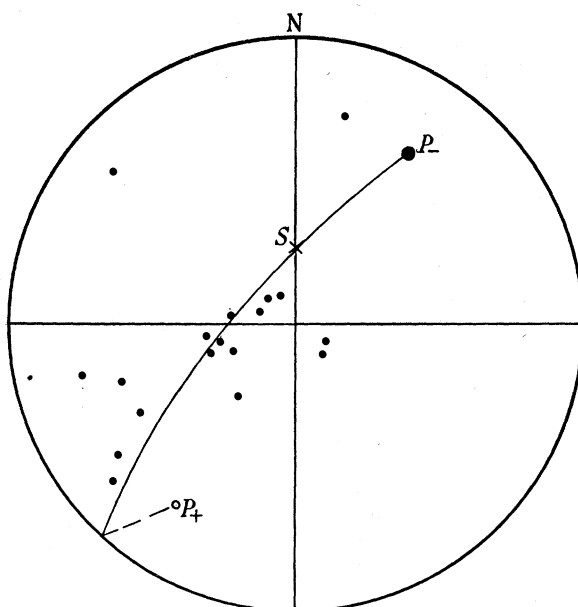


FIGURE 7. The mean directions of the n.r.m. of sample of Keuper Marl from Beachley, Gloucestershire. The primitive is the present horizontal. The bedding at this site is horizontal also.

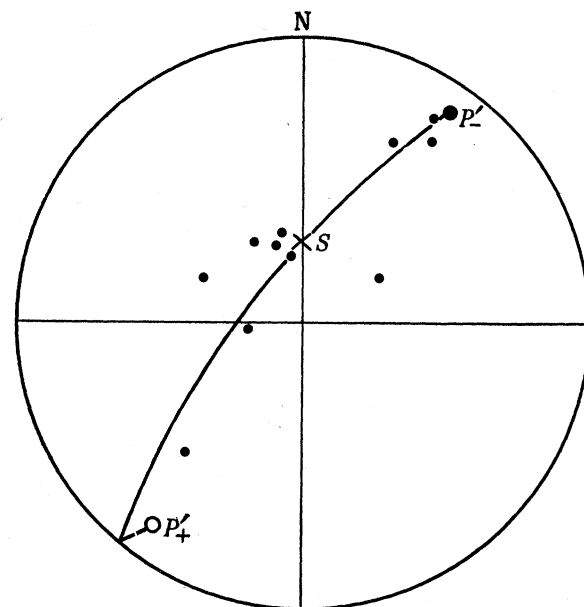


FIGURE 8. The mean directions of the n.r.m. of samples from the Tea Green Marls from Lavernock, Glamorganshire. The primitive is the present horizontal, but the beds dip by  $15^\circ$  at  $S31^\circ W$ .  $P'_-$  and  $P'_+$  are the tilted positions of  $P_-$  and  $P_+$  respectively.

The directions of magnetization of samples of Keuper Marl from Beachley in Gloucestershire and of five bands of chocolate marlstone from the Tea Green Marls at Lavernock in Glamorganshire are shown in figures 7 and 8 respectively. The directions are scattered about the great circles  $P_-SP_+$  and  $P'_-SP'_+$  respectively.

#### 6. SOME PROPERTIES OF THE I.R.M. PRODUCED BY SMALL FIELDS AT ROOM TEMPERATURE

Rock disks which had been stored in field-free space for 12 months were subjected to fields in the plane of the disks and were measured before and after the application of the field. A field  $h$  was applied for a time  $t'$  after which the decay of the intensity of the i.r.m. ( $M$ ) with time ( $t$ ) was observed. Two families of curves were obtained.

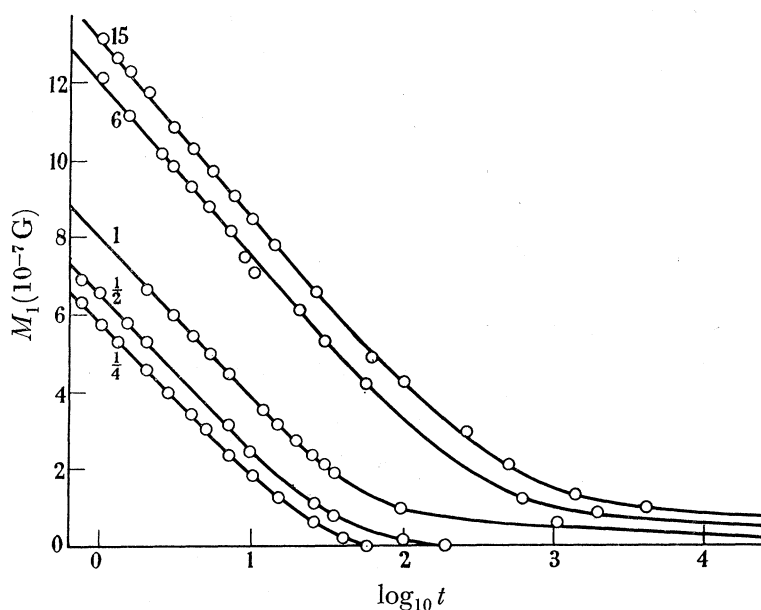


FIGURE 9. The decay characteristics of i.r.m.'s ( $M$ ) produced by a fixed field  $h$  applied for different times  $t'$ . The time  $t'$  in hours appropriate to each curve is given.  $t$  is measured in minutes.

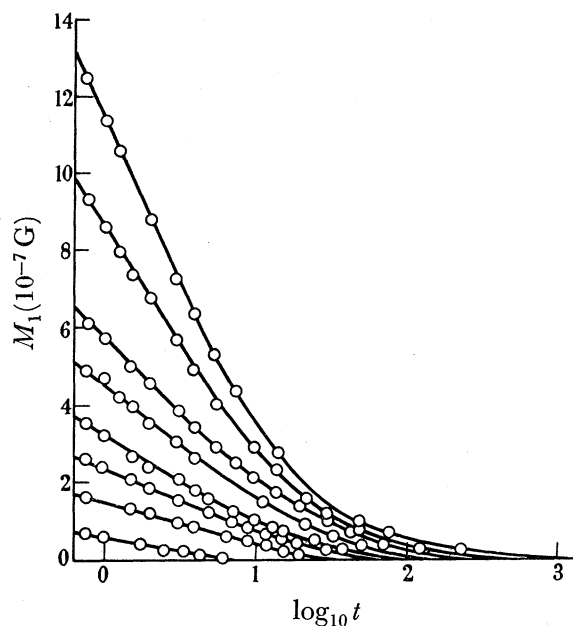


FIGURE 10. The decay characteristics i.r.m.'s ( $M$ ) produced by different fields  $h$  applied for a fixed time  $t'$ . Reading downwards the curves correspond to values of  $h$  equal to 10.70, 7.66, 5.13, 3.84, 2.56, 1.92, 1.28 and 0.64 respectively.  $t$  is measured in minutes.

#### (i) Dependence of i.r.m. ( $M$ ) on $t'$ with $h$ constant

The disk was placed in a field  $h=5.34$  G for times  $t'$  varying from 15 min to 15 h. In each case the decay curves were plotted. The family of curves so obtained is shown in figure 9.

#### (ii) Dependence of i.r.m. ( $M$ ) on $h$ with $t'$ constant

The family of decay curves for  $h$  varying from 0.64 to 10.70 G and  $t'=30$  min is shown in figure 10.

In figure 11,  $M_1$ , the intensity 1 min after removal from the field, is plotted against  $\log_{10} t'$ .

Figure 12 shows that  $dM/d(\log_{10} t)$  is proportional to  $h$ , and figure 13 that  $M_1$  is proportional to  $h$ .

Thus the i.r.m. of the Keuper Marl disk obeys the law

$$M = ah \log_{10} t' / t, \quad (6.1)$$

where  $a$  is a constant, provided that  $t$ ,  $t'$  and  $h$  are not too large.

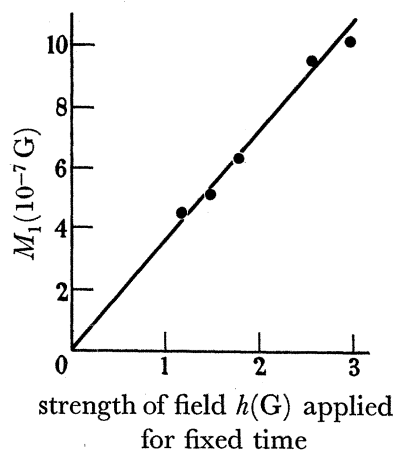


FIGURE 11. The relationship between intensity of the i.r.m. produced by a fixed field for varying times.

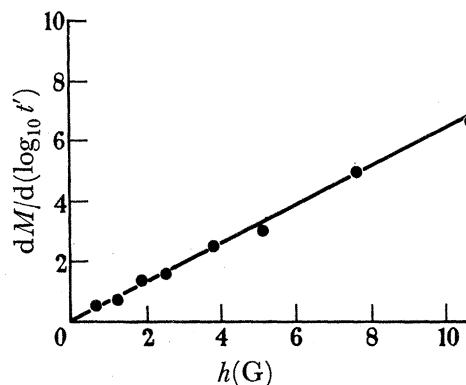


FIGURE 12. The relationship between the rate of decay of i.r.m.'s. and the field strength in which they were produced.

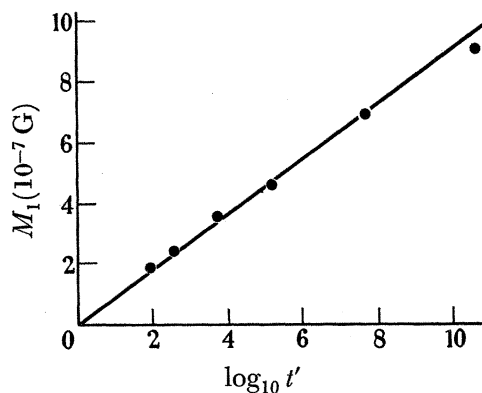


FIGURE 13. The relationship between the intensity of i.r.m.'s. produced by fields of different strengths applied for different times.

#### 7. THE TEMPORARY COMPONENT CONSIDERED AS AN I.R.M.

The temporary component (§ 3) had been built up in the geomagnetic field (of the order of 0.5 G) during 10 days and had decayed for 1 h. Thus from equation (6.1), taking  $a$  as found by the above experiments, the i.r.m. is found to be  $(1.88 \pm 0.12) \times 10^{-7}$  G.

As the measured value for  $T$  is  $(1.85 \pm 0.15) \times 10^{-7}$  G, the agreement is within the experimental limits of accuracy. This shows that equation (6.1) holds up to at least 10 days for fields of about  $\frac{1}{2}$  G.

#### 8. THE SECONDARY COMPONENT CONSIDERED AS AN I.R.M.

It is reasonable to suppose that the secondary component is also an i.r.m. built up by the present axial dipole field rather than a t.r.m. because the temperature of the rocks is unlikely to have been near the Curie points during the Quaternary. The rocks have been

exposed to an approximately constant field since its last reversal. By equation (6.1), it might be thought possible to determine this time. However, the rate of growth of i.r.m. will almost certainly fall off with respect to the logarithmic law over such a long period of time. Furthermore, the intensity of the secondary component cannot be assumed to have been zero when the last reversal of the main field occurred. Consequently, if the time which has elapsed since then is less than the period during which the main field was last reversed, some of the material contributing to the secondary component will not yet have had time to follow the change in sense of the main field and will still be reversely magnetized. Thus only a lower limit to the time  $t_r$  which has elapsed since the last geomagnetic reversal can be determined. Temperature fluctuations could also affect the intensity of the secondary component acquired in a given field according to whether the average temperature has been higher or lower than the mean temperature at the present time. Since the intensity of  $\mathbf{S}$  was that calculated 15 months after collection we have

$$\mathbf{S} = ah \log_{10} t_r / t. \quad (8.1)$$

Taking  $S$  and  $a$  as calculated in §§ 4 and 6, and remembering that throughout § 6 times were measured in minutes, we have  $\log_{10} t_r = 10.71 \pm 0.69$ , giving for  $t_r$  a value of 97 800 yr. The limits set to  $t_r$  by the standard error of  $\log_{10} t_r$  are 10 500 and 250 000 yr.

Hospers (1953, 1954) finds that the youngest Icelandic lavas showing reversed polarization are early Quaternary, which he estimates to be about 500 000 yr old. This would appear to give a maximum time during which the main field has maintained its present sense. The above result is quite consistent with this.

#### 9. DECAY OF TEMPORARY COMPONENT DURING MEASUREMENT

Since it takes a time of the order of 10 min to complete the measurements to determine the intensity and direction of magnetization of a rock disk, a temporary component acquired in storage will decay appreciably during measurement, unless it has been adequately aged. Suppose measurements are commenced at a time  $t_c$  min after removal from the field  $h$ .  $M(t_c)$  and  $M(t_c + 10)$  are the intensities of  $\mathbf{T}$  before and after the magnetometer measurements.

From equation (6.1), if  $t_c = 10$  min,  $M(t_c)/M(t_c + 10) = 1.3$ , and if  $t_c = 60$  min, the ratio is 1.04. The specimen should therefore be aged for such a time that the decay of  $\mathbf{T}$  during measurement is about equal to the accuracy to which intensities can be measured.

#### 10. STABILITY OF THE SECONDARY COMPONENT

Since this has been built up over such a long period of time it can possess a large intensity even when it has been aged for a year and the rate of decay is so small as to be undetectable during the experiments described above. Thus, although an i.r.m., it is apparently quite stable.

#### 11. NÉEL'S THEORY OF THE MAGNETIZATION OF SMALL SINGLE-DOMAIN PARTICLES

Néel (1949) describes how, for very small grains, the magnetic energy may be less than the energy of thermal fluctuations, i.e.

$$\frac{1}{2}vIh \ll \frac{1}{2}kT,$$

where  $v$  is the volume of grain,  $I$  is the spontaneous magnetization,  $h$  is the applied field,  $k$  is Boltzmann's constant and  $T$  is the absolute temperature. For such small particles Néel defines a time of relaxation  $\tau$  describing the rate at which complete thermodynamic equilibrium is established and which can be written as a function of the physical properties of the particles

$$\ln \tau = HIv/2 kT - \ln[3\lambda He/m (2E/\pi k)^{\frac{1}{2}}] - 0.5 \ln v/T. \quad (9.1)$$

$\lambda$  is the longitudinal magnetization,  $E$  is Young's modulus,  $H$  is the coercive force and  $e/m$  is the ratio of charge to mass of the electron. The following orders of magnitude for the physical quantities involved,  $\lambda=10^{-6}$ ,  $E=10^{12}$ ,  $H=10^3$  and  $I=2$  in e.m.u., give particle diameters and their approximate relaxation times as listed in table 5. The high coercivity of remanence of red and purple rocks (see table 7 in the preceding paper) and the diffuse diffraction lines shown in X-ray powder photographs suggest that the haematite cement is very fine grained, and it is possible that the particle diameters could range over the values calculated above. Larger 'particles' visible in thin sections under the microscope are possibly aggregates of very fine grains.

TABLE 5. CALCULATED RELAXATION TIMES OF HAEMATITE GRAINS

| diameter<br>of grain<br>( $\mu$ ) | relaxation<br>time |
|-----------------------------------|--------------------|
| 0.12                              | 1 sec              |
| 0.13                              | 10 min             |
| 0.15                              | 10 yr              |
| 0.16                              | 30 000 yr          |
| 0.17                              | 1 000 million yr   |

Néel also considers the properties of an assembly of grains all having the same spontaneous magnetization but different volumes  $v$  and different critical fields  $H$ . It is defined by the number  $n(Hv) dHdv$  of grains, the volume of which lies between  $v$  and  $v+dv$  and the critical fields of which lie between  $H$  and  $H+dH$ . To each grain there corresponds a point  $(v, H)$ . The loci of points on a  $v, H$  diagram having equal times of relaxation are approximately rectangular hyperbolae asymptotic to  $v=0$  and  $H=h$ , where  $h$  is the applied field. In a time  $\tau$  all those grains represented by points to the left of the hyperbola appropriate to a time of relaxation  $\tau$  become magnetized in the field  $h$ . A logarithmic law of the growth and decay of i.r.m. with time can be shown to hold for small fields. Departure from this law is accounted for by non-uniform density of points on the  $v, H$  diagram.

## 12. INTERPRETATION OF THE TEMPORARY AND SECONDARY COMPONENTS ON NÉEL'S THEORY

In figure 14 all the grains represented by points to the left of curve 1,  $\mathcal{H}(T_0 H_e t_r)$ , contribute to the intensity of  $\mathbf{S}_0$ , the 'virgin' value of the secondary component, where  $T_0$  is the average temperature of the rocks during the time  $t_r$  since the last reversal and  $H_e$  the average value of the earth's main field. During the 15 months before the measurement of  $\mathbf{S}$  (see §§ 4 and 5) all those grains to the left of curve 2,  $\mathcal{H}(T_0, 0, 15 \text{ months})$ , became demagnetized while the disk lay in field-free space. Only those grains between curves 1 and 2 contribute to  $\mathbf{S}$ .

The temporary components  $\mathbf{T}$  are created by grains, the representative points of which lie between curves 3,  $\mathcal{H}(T_0, H_e, 10 \text{ days})$  and 4,  $\mathcal{H}(T_0, 0, 1 \text{ h})$ .

The intensity of  $\mathbf{S}$  is unaffected by temporary components of magnetization built up over times of the order of the duration of laboratory experiments since the area of the  $v, H$  plane occupied by grains contributing to  $\mathbf{S}$  is out of reach of the  $\mathcal{H}$  curves appropriate to temporary magnetization.  $\mathbf{S}$  is created by grains having exclusively high times of relaxation, and  $\mathbf{T}$  by those grains having exclusively short times of relaxation.

Néel's theory thus explains the logarithmic growth and decay of the temporary component of magnetization. It explains qualitatively why the aged secondary component appears stable in character and indicates that both these components could be due to the fine-grained haematite cement.

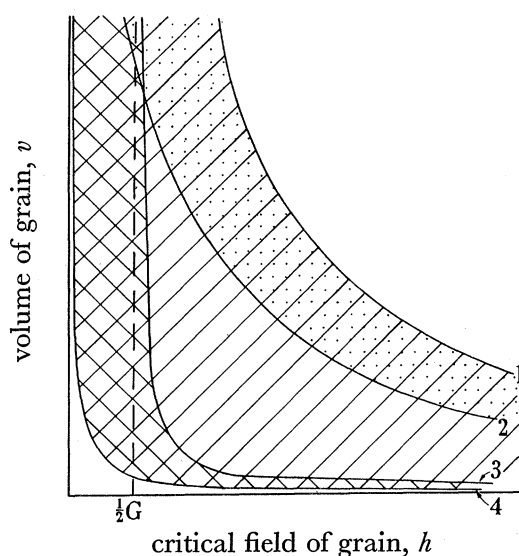


FIGURE 14.  $\mathcal{H}$ -curves for the different components of magnetization, curve 1 is  $\mathcal{H}(T_0, H_e, t_r)$ , curve 2 is  $\mathcal{H}(T_0, H_e, 10 \text{ days})$ , curve 3 is  $\mathcal{H}(T_0, 0, 1 \text{ h})$  and curve 4 is  $\mathcal{H}(T_0, 0, 15 \text{ months})$ .

### 13. CONTRIBUTION TO N.R.M. OF GRAINS HAVING VERY HIGH RELAXATION TIMES

The relation between grain diameter and relaxation time, shown in table 5, is such that if the grain size of the red haematite cement is of the right order to account for the effects discussed in this paper in terms of Néel's single-domain theory, grains having times of relaxation much greater than those previously considered will also be present.

#### (a) *A possible origin of the primary component of n.r.m.*

If the red cement was initially unmagnetized, those grains the times of relaxation of which are greater than the age of the rock are of no further interest. However, if the red cement became magnetized along the axis of the ancient geomagnetic field when it was precipitated, such grains will have retained that direction of magnetization. The view generally held by geologists is that the red staining appeared soon after deposition.

#### (b) *Possible components of n.r.m. due to other ancient geomagnetic fields*

In the final paper of this series the stable directions of n.r.m. of rocks of different ages are interpreted in terms of a slow wandering of the poles throughout geological time. It is shown that the rate of polar wander is very small compared with the average frequency of reversal of the geomagnetic field.

The Sidmouth Marls can therefore be considered to have experienced an alternating geomagnetic field the direction of which has slowly rotated.

Thus grains having times of relaxation greater than the average times between reversal will be unorientated. Those having times of relaxation less than this will contribute either to the secondary or to the temporary components of magnetization previously discussed.

#### 14. A SUGGESTED TEST OF STABILITY

The stability of magnetization of a rock depends on the relative strengths of the primary, secondary and temporary components. Experiments of the kind described in § 6 demonstrate whether the i.r.m. of the rock obeys equation (6.1). If this is so, the constant  $a$  can be evaluated, but it is not necessary to repeat the whole procedure for every specimen in order to calculate the intensities of the temporary components or to estimate an upper limit for the intensity of the secondary component.

If the measured intensity of the total n.r.m. is much greater than the calculated intensities of the secondary and temporary components, the n.r.m. will be stable. Such was the case for the stable rocks described in the paper IV. Many samples can be tested in this manner within a day.

#### REFERENCES

- Clegg, J. A., Almond, M. & Stubbs, P. 1954 *Phil. Mag.* (7), **45**, 583–598.  
 Dewey, H. 1948 *British Regional Geology, South West England*. London: H.M.S.O.  
 Fisher, Sir R. A. 1953 *Proc. Roy. Soc. A*, **217**, 295–305.  
 Hospers, J. 1953 *Proc. Acad. Sci. Amst. B*, **56**, 467–491.  
 Hospers, J. 1954 *Proc. Acad. Sci. Amst.* **57**, 112–121.  
 Irving, Rev. A. 1888 *Quart. J. Geol. Soc. Lond.* **44**, 149–163.  
 Néel, L. 1949 *Ann. Géophys.* **5**, 99–136.  
 Ussher, W. A. E. 1876 *Quart. J. Geol. Soc. Lond.* **32**, 274–277.